Nonlinear Dyn (2011) 64: 279–292
DOI 10.1007/s11071-010-9860-x

ORIGINAL PAPER

A robust method on estimation of Lyapunov exponents from a noisy time series

Caixia Yang · Christine Qiong Wu

Received: 9 February 2010 / Accepted: 30 September 2010 / Published online: 23 October 2010

Abstract Lyapunov exponents can indicate the asymptotic behaviors of nonlinear systems, and thus can be used for stability analysis. However, it is notoriously difficult to estimate these exponents reliably from experimental data due to the measurement error (noise). In this paper, a novel method for estimating Lyapunov exponents from a time series in the presence of additive noise corruption is presented. The method combines the ideas of averaging the noisy data to form new neighbors and of nonlinear mapping to determine neighborhood mapping matrices. Two case studies of balancing control of a bipedal robot and the Lorenz systems are presented to demonstrate the efficacy of the proposed method. The bipedal robot system has two negative Lyapunov exponents while the Lorenz system has one positive, zero, and negative exponents, respectively. It is shown that, as compared with the existing methods, our proposed one is more robust to the ratio of signal to noise, and is particularly effective in estimating negative Lyapunov exponents. We believe that the work can contribute significantly to the stability analysis of nonlinear systems using a noisy time series.

C. Yang · C.Q. Wu (✉)
Department of Mechanical and Manufacturing Engineering, University of Manitoba, Winnipeg, MB, R3T 5V6, Canada
e-mail: cwu@cc.umanitoba.ca

Keywords Stability analysis · Lyapunov exponents · Noisy time series · Nonlinear mapping

1 Introduction

Lyapunov's stability theory is of central importance for the stability analysis of nonlinear systems, especially of robotic control systems. The core of Lyapunov's stability analysis is the derivation of a Lyapunov function. However, there is no constructive method available for such a derivation. Consequently, stability of many nonlinear systems cannot be analyzed. Lyapunov exponents, defined as the average exponential rates of divergence or convergence of nearby orbits in the state space, can indicate system stability [1–3]. As compared to its counterpart of Lyapunov's second method, the main advantage of the concept of Lyapunov exponents is that the methods for estimating the exponents are constructive, which makes the stability analysis of complex nonlinear systems possible. Since, for complicated systems, it is in general impossible to determine Lyapunov exponents analytically, we can estimate them numerically using either a mathematical model or a time series. The results can characterize the system stability provided that the numerical artifact is under control [4].

Methods for estimating Lyapunov exponents based on a mathematical model have been well developed [1, 3, 5, 6] and widely used for diagnosing chaotic systems. In addition, Lyapunov exponents have also been

used for the stability analysis of complex nonlinear systems, as discussed in detail in [7–13] and the references cited in our previous work [14]. However, when considering real world physical systems, those crucial differential equations are not always known. Even if the models are available, due to their complexities and uncertainties, the estimation of Lyapunov exponents can be unfeasible [13–16].

A time series is a sequence of observations which are ordered in time. Since a single experimental time series is affected by all of the relevant dynamical variables, it contains a relatively complete historical record of the dynamics. The work of Takens [17] shows that the complete dynamics of a system can be constructed from a suitable single time series derived from that system; therefore, an algorithm for extracting Lyapunov exponents of a system from such a time series is possible and highly desirable. The most attractive advantage of using a time series is that the data for only one state is required, which can often be measured experimentally. Due to the above advantage, estimation of Lyapunov exponents from a time series is extremely attractive for the analysis of large and unknown complex systems, such as biological systems [18–23]. An excellent review of the applications of Lyapunov exponents to biomedical applications has been published by Dingwell [24].

There are two challenges when estimating Lyapunov exponents using a time series. One challenge is that the available methods for estimating Lyapunov exponents based on a time series are for chaotic systems where at least one exponent is positive. These methods are not reliable for stable systems where all Lyapunov exponents are zero or negative [1]. Reliable estimation of negative Lyapunov exponents may not be crucial for diagnosing chaotic systems since positive exponents are of interests. However, it is extremely important for the analysis of stable systems, especially those of which all exponents are negative. To address this challenge, in our previous work [14], an improved method was proposed for estimating negative Lyapunov exponents from a time series using nonlinear mapping to form neighborhood matrices. The results have shown that our method has three advantages over those based on linear mapping, in that (1) the accuracy of the negative Lyapunov exponents estimated using nonlinear mapping is improved as compared with those from linear mapping; (2) the Lyapunov exponents are less sensitive to the parameters, such as the time lag and the evolve time; and (3) since Taken's theorem on embedding dimension is often required for linear mapping, spurious exponents are generated. However, when nonlinear mapping is used, the number of spurious exponents can be significantly lower than the one from linear mapping. If the system dimension is known, e.g., the robotic system shown in the first case study, no spurious Lyapunov exponent is generated since the embedding dimension can be chosen the same as the system dimension.

Another challenge of using a time series for estimating Lyapunov exponents is that it is inevitable to have measurement noise in the measured time series. The presence of such noise has adverse effects on the quality of the estimated Lyapunov exponents since the accuracy of the neighborhood matrix is degraded, and the chance of picking a false neighbor is increased. Several methods for determining Lyapunov exponents using a noisy time series for chaotic systems have been developed [1, 3, 25–32]. Among them, Zeng et al. [29] proposed a method aiming at using a short time series of low precision for determining Lyapunov exponents, where a concept of "a shell" to minimize the effects of noise was proposed. Their "shell" was formed by inner and outer hyper-spheres, which were determined by the nature and the level of noise. It was believed that effects of noise were high for the neighbors too close to, as well as too far from, the trajectory points. Thus, the neighboring vectors falling in the "shell" were believed with low effects from noise, and were used for determining the neighborhood matrices. Banbrook et al. [33] proposed a method of defining a neighborhood matrix using a noisy time series where the average of the selected neighbors was used for each entry in the neighborhood matrix. To demonstrate the effectiveness of their method, they included results using all the noise robustness measures suggested by Darbyshire and Broomhead [34]. Banbrook et al. [33] believed that averaging the neighboring vectors tends to reduce the effects of noise, and thus improves the performance of their method in comparison to the conventional ones. However, in the reference [33], the neighborhood matrix was defined differently from the conventional way, and the rationale for their definition was not discussed. We also found that the method by Banbrook et al. [33] has a limitation on the number of the sub-groups, i.e., the number of the sub-groups should be an even number. Otherwise, the estimation procedure could not be implemented. Thus it is imper-

ative to develop methods robust to noise involved in the time series.

In this work, we propose a new method for estimating Lyapunov exponents using a noisy time series. Although not restricted to negative Lyapunov exponents, we are especially interested in estimating negative exponents using noisy time series for systems of which all exponents are negative. We combine our previous work of nonlinear mapping with the ideas of (1) setting an inner hyper-sphere to exclude the neighbors too close to the fiducial trajectory point, where the effects of noise are believed high, and (2) averaging the neighboring vectors to form a new neighboring vector for determining the neighborhood mapping matrix. Furthermore, we follow the conventional definition of neighbors, i.e., all vectors are measured from the central point, or on the evolved central point [1]. Note that different from Zeng's method [29], the outer hyper-sphere is not used in order to obtain enough nearest neighbors required for nonlinear mapping.

The effectiveness of the proposed method is demonstrated through two case studies of a balancing biped during standing and the Lorenz system. In the bipedal system, the biped is simplified as an inverted pendulum attached to a foot-link. A control torque is applied at the ankle joint to keep the biped at the upright position. The foot-link is stationary on the ground, rather than pinned to the ground. Thus, three constraints between the foot-link and the ground (no lifting, no slipping and no rolling over) must be satisfied. Such a requirement makes the stability analysis of the balancing control system, using a Lyapunov function, difficult (please see details in [16, 37]). For the Lorenz system, the same parameters are used as those in Zeng's work [28]. A time series from each system is first generated from the mathematical model by the numerical integration using fourth-order Runge–Kutta integration. In this work, the effect of an additive noise component on the data set is considered. Thus, the second time series is obtained by adding independent identically distributed Gaussian white noise to the time series produced by the mathematical model. Such a noisy time series is used for estimating Lyapunov exponents in this work. Gaussian white noise is of special interest here since it is the type of measurement noise commonly encountered in experimental situations, especially for mechanical systems [34]. Lyapunov exponents are then estimated using (1) the mathematical model, and (2) a noisy time series, where the method developed by Banbrook et al. [33] and our proposed method are employed. To demonstrate the role of nonlinear mapping, with the same time series both the linear map and a second-order nonlinear map are employed. All of these results are compared with those estimated from the mathematical model. In the estimation of Lyapunov exponents, the selection of several parameters, such as the time delay, evolution time and embedding dimensions, can affect the estimated exponents significantly [3, 35]. In this work, the time delays were determined by the first zero crossing of the autocorrelation method [14]. The selections of the embedding dimension and the evolution time are discussed later.

2 Mathematical preliminary

2.1 The concept of Lyapunov exponents

Lyapunov exponents, λ_i $(i = 1, \ldots, n)$, are the average exponential rates of divergence or convergence of nearby orbits in the state space. Wolf et al. [1] defined the spectrum of Lyapunov exponents in the manner most relevant to spectral estimations. Given a continuous dynamical system in an n-dimensional phase space, we monitor the long-term evolution of an infinitesimal n-sphere of initial conditions; the sphere will become an n-ellipsoid due to the locally deforming nature of the flow. The ith one-dimensional Lyapunov exponent is then defined in terms of the length of the ellipsoidal principal axis $\|\delta x_i(t)\|$:

$$\lambda_i = \lim_{t\to\infty} \frac{1}{t} \ln \frac{\|\delta x_i(t)\|}{\|\delta x_i(t_0)\|} \quad (i = 1, \ldots, n), \tag{1}$$

where λ_i are ordered from the largest to the smallest. The $\|\delta x_i(t)\|$ and $\|\delta x_i(t_0)\|$ denote the lengths of the ith principal axes of the infinitesimal n-dimensional hyper-ellipsoids at final and initial times, t and t_0, respectively. Thus, Lyapunov exponents are related to the expanding or contracting nature of different directions in phase space. Since the orientation of the ellipsoid changes continuously as it evolves, the directions associated with a given exponent vary in a complicated way through the attractor. Therefore, one cannot speak of a well-defined direction associated with a given exponent.

The concept of Lyapunov exponents provides a generalization of the linear stability analysis of nonlinear dynamic systems. Lyapunov exponents are global

properties and are independent of the trajectory chosen to estimate them (the fiducial trajectory). This independence is a consequence of a theorem of Oseledec [6], which applies in the limit of infinite time. However, in practical applications, we deal with finite-time Lyapunov exponents, which are defined as

$$\lambda_i = \frac{1}{T} \ln \frac{\|\delta x_i(t)\|}{\|\delta x_i(t_0)\|} \quad (i = 1, \ldots, n). \tag{2}$$

In the limit, as $t \to \infty$, the finite-time Lyapunov exponents converge to the true Lyapunov exponents [29]. The exponents, λ_i, can be ordered as $\lambda_1 \geq \lambda_2 \geq \cdots \geq \lambda_k$, which gives the spectrum of Lyapunov exponents. These exponents are independent of the initial conditions if the system is ergodic [6].

2.2 Noise levels

In this work, additive Gaussian white noise is considered. The noise level has often been represented by the signal-to-noise ratio (SNR) and the percentage of noise. The white noise was scaled by an appropriate factor in order to achieve a desired signal-to-noise ratio. The signal-to-noise ratio is defined as

$$\mathrm{SNR(dB)} = 20 \log_{10}(A_{\mathrm{signal}}/A_{\mathrm{noise}}), \tag{3}$$

where A is the root mean square, which is a statistical measure of the magnitude of a varying quantity. The percentage of noise is defined as

$$\mathrm{Noise}(\%) = A_{\mathrm{noise}}/A_{\mathrm{signal}} \times 100. \tag{4}$$

The percentage of noise varies upon the measured signals. For robots consisting of close-to-rigid links, the percentage of noise can be easily controlled below 2%.[1] When the percentage of noise is greater than 5%, the measured values would be considered unreliable. Correspondingly, an SNR greater than 35 dB can be regarded as low noise and an SNR less than 25 dB as high noise. In this work, the noise level between 1 and 5% (SNR from 25 to 40 dB) is selected to investigate the effects of noise on the values of Lyapunov exponents for the first case. We added Gaussian white noise to simulated data similarly to how Brown and Bryant did in [35] for their second case.

[1] See http://www.posital.com/us/products/POSITAL/AbsoluteInclinometers/AbsoluteInclinometers_base.html?gclid=COff3_GO4J0CFSDxDAodiQLRNw.

3 Methodology

3.1 Estimation of Lyapunov exponents based on a time series using linear mapping

When dealing with a time series $x_i = x(i\Delta t)$ $(i = 1, 2, \ldots, N)$, where N is the number of observations and Δt is the time interval between measurements, the procedure of estimating Lyapunov exponents from a time series includes the following steps [20, 39]:

1. Reconstructing the dynamics in a finite dimensional phase space: Choose an embedding dimension d_E and reconstruct a d_E-dimensional orbit representing the time evolution of the system using delay coordinates to form the vectors:

$$y_i = \left(x_i, x_{i+T_{\mathrm{lag}}}, \ldots, x_{i+(d_E-1)T_{\mathrm{lag}}}\right)^T, \tag{5}$$

   where T_{lag} is the time lag. Equation (5) provides the fiducial trajectory for the estimation of Lyapunov exponents.
2. Determining the neighbors $y^r(n)$ of each fiducial trajectory point $y(n)$: for each fiducial trajectory point $y(n)$, consider the hyper-sphere centered at $y(n)$ of the radius $r_{\min}$, which is selected based on trial and error in this work to obtain accurate Lyapunov exponents. Consider the set of trajectory points $y^r(n)$ such that:

$$\left\| y^r(n) - y(n) \right\| \geq r_{\min}. \tag{6}$$

   Note that differently from Zeng's method [29], the outer hyper-sphere is not used in order to obtain enough nearest neighbors for nonlinear mapping.
3. Determining the $d_E \times d_E$ matrix J_i which describes how the time evolution sends vectors around $y(n)$ to vectors around $y(n+m)$: After a time $m\Delta t$, the vectors $(y^r(n) - y(n))$ evolve to the vectors $(y^r(n+m) - y(n+m))$. Suppose that the evolution of $y(n)$ is given by the map $y(n+m) = F(y(n))$, the matrix J_i corresponding to linear mapping is obtained by looking for neighbors $y^r(n)$ of $y(n)$, and imposing

$$J_i\left(y^r(n) - y(n)\right) \approx y^r(n+m) - y(n+m). \tag{7}$$

   The elements of J_i are obtained by a least-squares fit (refer to description in [14] for details).

4. Determining Lyapunov exponents: A sequence of matrices $J_1, J_2, J_3, \ldots$ is obtained from Step 3. Using QR decomposition, one can determine successively orthogonal matrices $Q_{(j)}$ and upper triangular matrices $R_{(j)}$ with positive diagonal elements such that $Q_{(0)}$ is the identity matrix and

$$\begin{aligned} &J_1 Q_{(0)} = Q_{(1)} R_{(1)}, \\ &J_2 Q_{(1)} = Q_{(2)} R_{(2)}, \\ &\vdots \\ &J_{j+1} Q_{(j)} = Q_{(j+1)} R_{(j+1)}. \end{aligned} \tag{8}$$

This decomposition is unique except in the case of zero diagonal elements. Then Lyapunov exponents λ_K^i are given by

$$\lambda_K^i = \frac{1}{TK} \sum_{j=0}^{K-1} \ln R_{(j)ii}, \tag{9}$$

where K is the available number of matrices, T is sampling time step, $i = 1, 2, \ldots, d_E$.

5. Repeat Steps 2 through 4 along the fiducial trajectory until the convergent Lyapunov exponents are achieved.

3.2 Estimation of Lyapunov exponents based on a time series using nonlinear mapping

In most previous work, the linear Taylor series expansion, shown in (7), was used to generate the local neighborhood-to-neighborhood map of the embedding chaotic systems. It has been stated that linear mapping prevents the applicability of the methods for estimating negative Lyapunov exponents [1, 30, 35, 36]. This is a significant restriction to the concept of Lyapunov exponents for analyzing stable systems, of which the exponents are negative or zero. Linear mapping is not reliable for estimating negative exponents because the displacement due to the local data-set curvature is comparable to the thickness of the data set, which occurs in stable systems with all exponents being negative or zero [1, 30, 35, 36]. In principle, using higher-order expansions, the local neighborhood-to-neighborhood map contains more information of the underlying dynamical system than just using the local linear map, and more accurate descriptions of the system can be achieved. Thus, we propose to use nonlinear expressions, i.e., the higher-order expansions instead of the linear expression, for obtaining the local neighborhood-to-neighborhood map of the embedding potentially stable engineering systems.

In the Taylor series expansion, the relationship between the order of the Taylor series N_{Tay}, the embedding dimension of the phase space d_E, and the minimum number of parameters N_p is given by the following equation [39]:

$$N_p = \left[\prod_{k=1}^{N_{\text{Tay}}} \frac{d_E + k}{k} \right] - 1 = \frac{(d_E + N_{\text{Tay}})!}{d_E! N_{\text{Tay}}!} - 1. \tag{10}$$

From (10) we observe that N_p grows rapidly with the order of Taylor series N_{Tay} and the dimension of the reconstructed phase space d_E. N_p is also the minimum number of neighbors required to estimate the values for the fitted parameters in the expansion. Using less than N_p neighbors would result in an underdetermined least-squares fit. This also means that as the embedding dimension of the system and the order of the Taylor series increase, the amount of data required to find N_p appropriate neighbors will also increase proportionally.

For a fiducial orbit $y(n)$, its rth neighbor is defined as $y^r(n)$, the small displacement between $y^r(n)$ and $y(n)$ is represented by $Z^r(n; T_0)$, after time-step T_1; the small displacement is represented by $Z^r(n; T_1)$. In the embedding phase space, $Z^r(n; T_1)$ has d_E components.

Let $Z_\alpha^r(n; T_1)$ be the αth component of $Z^r(n; T_1)$. Expanding the local neighborhood-to-neighborhood map F (which is a nonlinear function) in a Taylor series about the fiducial orbit $y(n)$, we find

$$\begin{aligned} Z_\alpha^r(n; T_1) = {} & DF_{\alpha\beta}(n) Z_\beta^r(n; T_0) \\ & + DF_{\alpha\beta\gamma}^{(2)}(n) Z_\beta^r(n; T_0) Z_\gamma^r(n; T_0) \\ & + \cdots \end{aligned} \tag{11}$$

where

$$DF_{\alpha\beta}^{(2)}(n) = \frac{\partial F_\alpha}{\partial F_\beta}, \tag{12a}$$

$$DF_{\alpha\beta\gamma}^{(2)}(n) = \frac{1}{2!} \frac{\partial^2 F_\alpha}{\partial y_\beta \partial y_\gamma}. \tag{12b}$$

In summary, we can get the common form of matrix J for any dimension d_E as follows:

$$\begin{aligned} &J_{k,l} = \partial F_{kl} + \frac{1}{2} \sum_{\alpha=1}^{d_E} \partial F_{kl\alpha} Z_\alpha^r, \\ &k, l = 1, \ldots, d_E. \end{aligned} \tag{13}$$

Once the matrix J at each time instant is determined, Lyapunov exponents are obtained using (8) and (9).

In this work, the second-order mapping, i.e., if the order of Taylor series N_{Tay} is equal to 2, is used for constructing the mapping matrices J. The derivation will be presented in detail in the Appendix where the dimension of the reconstructed phase space d_E is equal to 2, as the case studied is a two-dimensional system.

3.3 Averaging method for reducing the noise influence

The idea of averaging the neighboring vectors is shown through the following formulation:

$$
\begin{aligned}
\tilde{Z}^1(n;T_0) &= \big(\big(y^1(n)-y(n)\big)+\big(y^2(n)-y(n)\big)+\cdots \\
&\quad +\big(y^{(M/N_p)}(n)-y(n)\big)\big)/(M/N_p), \\
\tilde{Z}^2(n;T_0) &= \big(\big(y^{(M/N_p)+1}(n)-y(n)\big) \\
&\quad +\big(y^{(M/N_p)+2}(n)-y(n)\big)+\cdots \\
&\quad +\big(y^{2(M/N_p)}(n)-y(n)\big)\big)/(M/N_p), \\
\tilde{Z}^3(n;T_0) &= \big(\big(y^{2(M/N_p)+1}(n)-y(n)\big) \\
&\quad +\big(y^{2(M/N_p)+2}(n)-y(n)\big)+\cdots \\
&\quad +\big(y^{3(M/N_p)}(n)-y(n)\big)\big)/(M/N_p), \\
&\vdots \\
\tilde{Z}^{N_p}(n;T_0) &= \big(\big(y^{(N_p-1)(M/N_p)+1}(n)-y(n)\big) \\
&\quad +\big(y^{(N_p-1)(M/N_p)+2}(n)-y(n)\big)+\cdots \\
&\quad +\big(y^{N_p(M/N_p)}(n)-y(n)\big)\big)/(M/N_p),
\end{aligned}
\tag{14}
$$

where $y(n)$ is the nth centered point, while $y^r(n)$ is the noisy rth neighbor of the central point $y(n)$, M is the total number of noisy neighbors of the central point $y(n)$ on fiducial trajectory, and N_p is the number of sub-groups, which is equal to the minimum number of the neighbors required to estimate the values for the fitting parameters in the expansion. Note that $\tilde{Z}^r(n;T_0)$ in (14) represents the neighboring vectors, which is equivalent to $Z^r(n;T_0)$ described in Sect. 3.2, except that the effects of noise have been compensated using the averaging procedure.

After applying the averaging procedure, a sequence of neighboring vectors is obtained, which corresponds to $(y^r(n)-y(n))$ in Step 3 of Sect. 3.1, with the effects of noise reduced. To obtain accurate Lyapunov exponents, the inner radius in this work was selected based on trial and error.

Additive Gaussian white noise is considered here, and an average of a number of vectors will tend to reduce the effects of such noise. All vectors are measured from the central point, or on the evolved central point, which is directly based on Wolfs' definition. In addition, our averaging method eliminates the limitation on the number of the sub-groups.

3.4 Case studies

Two distinguished case studies are presented here. For the first case study, balancing control of a biped during standing is presented, where all Lyapunov exponents are negative. For the second case study, the Lorenz system is presented, where the system has one positive, one zero and one negative Lyapunov exponents. We demonstrate that the method proposed in this work can estimate negative Lyapunov exponents and improve the accuracy of positive exponents.

3.4.1 Case study 1

A balancing bipedal robot during standing is used as a case study to demonstrate the effectiveness of our proposed method. The time series is first generated by the mathematical model. Independent identically distributed Gaussian white noise is added to the time series, which simulates the kind of measurement noise commonly encountered in experimental situations [34].

A bipedal robot during standing is simplified as a two-link bipedal model including a foot-link, which provides a base of support on the ground and an inverted pendulum representing the legs, trunk, arms and head, as shown in Fig. 1(a). The feet position is assumed to be bilaterally symmetric and stationary, and the biped moves in the sagittal plane [16, 37]. Free-body diagrams of the inverted pendulum and the foot-link are shown in Fig. 1(b) and (c) respectively.

Three dynamic equations of the inverted pendulum are developed using the Euler–Lagrangian equation as:

$$\tau = mgr\sin\theta - \big(I+mr^2\big)\ddot{\theta}, \tag{15a}$$

$$F_{ax} = mr\dot{\theta}^2\sin\theta - mr\ddot{\theta}\cos\theta, \tag{15b}$$

$$F_{ay} = mr\dot{\theta}^2\cos\theta + mr\ddot{\theta}\sin\theta - mg, \tag{15c}$$

where F_{ax} and F_{ay} are the horizontal and vertical force components respectively between the foot-link and the

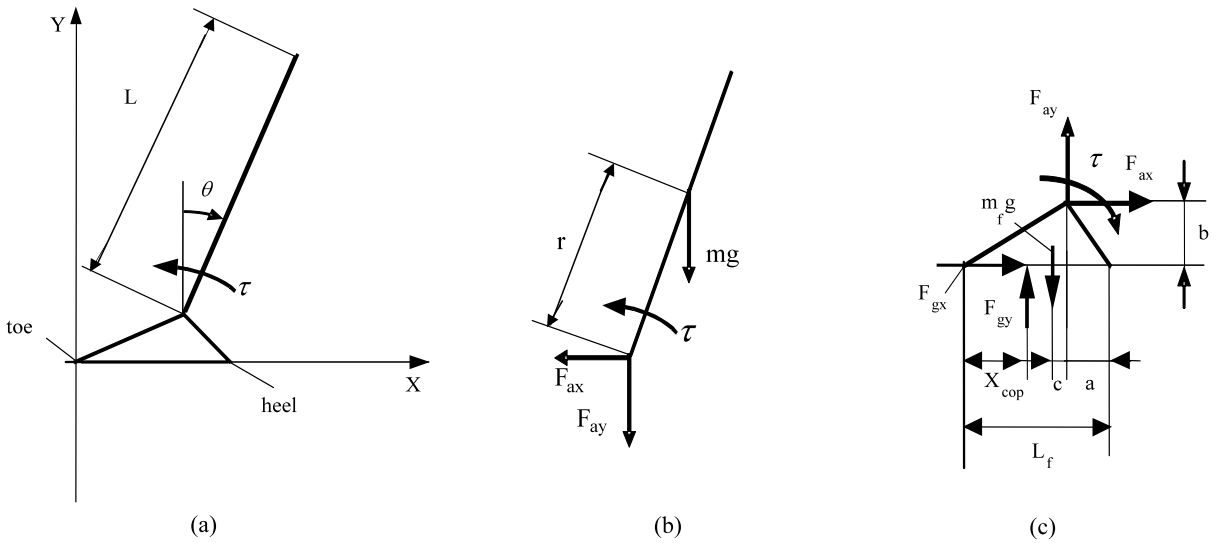

Fig. 1 (**a**) A simplified bipedal model consisting of an inverted pendulum moving in the sagittal plane and a rigid foot-link, which is not fixed on the ground but remains stationary. Control torque acting at the ankle stabilizes the inverted pendulum to upright position, (**b**) free body diagram of the inverted pendulum, and (**c**) free body diagram of the foot-link

inverted pendulum, i.e. at the ankle joint. As shown in Fig. 1, $\tau, \theta, \dot{\theta}$ and $\ddot{\theta}$ are the ankle torque (counterclockwise as "+"), angular displacement, velocity and acceleration of the body (clockwise as "+"), respectively. The parameters r, L, m and I are the distance between the center of mass of the pendulum and the ankle, length of pendulum, mass of the body and the moment of inertia of the pendulum about the mass center, respectively. The origin of the fixed coordinate system is located at the toe. The x-axis is pointing horizontally from the toe to the heel, and the y-axis is upward.

Since the foot-link is static, three equilibrium equations are:

$$F_{ax} = -F_{gx}, \tag{16a}$$

$$F_{ay} = m_{\mathrm{f}} g - F_{gy}, \tag{16b}$$

$$F_{gy}(L_{\mathrm{f}} - a - x_{\mathrm{cop}}) + m_{\mathrm{f}} g c - F_{gx} b - \tau = 0. \tag{16c}$$

The F_{gx} and F_{gy} are the horizontal and vertical ground reaction forces, respectively. The parameters a, c, b, x_{cop}, L_{f}, m_{f} and m are the horizontal distance between the ankle and the heel, between the foot mass center and the ankle, ankle height, distance between the pressure center and the toe, foot length, mass of the feet and mass of the body, respectively.

By eliminating the ankle forces, F_{ax} and F_{ay} from (15) and (16), the dynamic equations for the bipedal system become

$$\tau = mgr \sin\theta - (I + mr^2)\ddot{\theta}, \tag{17a}$$

$$F_{gx} = mr\ddot{\theta}\cos\theta - mr\dot{\theta}^2 \sin\theta, \tag{17b}$$

$$F_{gy} = (m_{\mathrm{f}} + m)g - mr\ddot{\theta}\sin\theta - mr\dot{\theta}^2\cos\theta. \tag{17c}$$

Unlike many of the previous papers, in this work, the foot-link is not fixed on the ground, but is required to be stationary. Since the roll-over constraint is equivalent to the center of pressure (COP) constraint as the foot-link is on level ground [38], three constraints are considered. The gravity constraint requires that the vertical ground force (F_{gy}) be upward. The friction constraint requires that the horizontal ground force (F_{gx}) be lower than the maximum static friction. The COP constraint requires that the pressure center (x_{cop}) be between the toe and the heel, indicating that the rotation about the toe or the heel does not occur. The three constraints are written as

$$F_{gy} \geq 0, \tag{18a}$$

$$|F_{gx}| \leq \mu F_{gy}, \tag{18b}$$

$$0 \leq x_{\mathrm{cop}} \leq L_{\mathrm{f}}. \tag{18c}$$

From (18c), the pressure center (x_{cop}) is

$$x_{\mathrm{cop}} = L_{\mathrm{f}} - a - \frac{bF_{gx} - \tau + cm_{\mathrm{f}}g}{F_{gy}}. \tag{18d}$$

These constraints impose bounds to the control torque, which change with the states of the system. The determination of the control bounds was presented in our previous work [16, 37]. The control bounds imposed on the control torque, due to the constraints, have significant effect on designing balance control laws. Such bounds make the control design and the stability analysis highly challenging [37]. A PD-based switching state feedback control law is designed to stabilize the biped at the upright position while keeping the foot-link stationary. The controller considers each constraint, shown in inequalities (18), and determines the maximum and minimum feasible torque necessary to satisfy the constraints between the foot-link and the ground. The controller is a simple PD control as the control torque is within the control bounds, and it takes the value of the control bounds as it reaches the bounds. The controller is shown as:

$$\tau = \begin{cases} \tau_{\text{PD}} & \text{if } \tau_{\text{lower}} \le \tau_{\text{PD}} \le \tau_{\text{upper}} \\ \tau_{\text{upper}} & \text{if } \tau_{\text{PD}} \ge \tau_{\text{upper}} \\ \tau_{\text{lower}} & \text{if } \tau_{\text{PD}} \le \tau_{\text{lower}} \end{cases} \tag{19}$$

where $\tau_{\text{PD}} = -k_{\text{P}}\theta - k_{\text{D}}\dot{\theta}$, the upper bound τ_{upper} and the lower bound τ_{lower} depend on the states, i.e., θ and $\dot{\theta}$, which have been determined from our previous work [16].

The state-space model of the system is derived by defining the state vector $x = \{\theta, \dot{\theta}\}^T = \{x_1, x_2\}^T$ and combining (19) with (17a):

$$\dot{x} = f(x) = \begin{cases} f_1(x) = \left\{ \dfrac{x_2}{\frac{mgr\sin x_1 - \tau_{\text{PD}}}{M}} \right. \\ \quad \text{if } \tau_{\text{lower}} \le \tau_{\text{PD}} \le \tau_{\text{upper}} \end{cases} \quad \text{(Region 1)}$$

$$\begin{cases} f_2(x) = \left\{ \dfrac{x_2}{\frac{mgr\sin x_1 - \tau_{\text{upper}}}{M}} \right. \\ \quad \text{if } \tau_{\text{PD}} \ge \tau_{\text{upper}} \end{cases} \quad \text{(Region 2)}$$

$$\begin{cases} f_3(x) = \left\{ \dfrac{x_2}{\frac{mgr\sin x_1 - \tau_{\text{lower}}}{M}} \right. \\ \quad \text{if } \tau_{\text{PD}} \le \tau_{\text{lower}} \end{cases} \quad \text{(Region 3)} \tag{20}$$

The above 2-dimensional state-space model leads to two Lyapunov exponents. The stability of the above control system has been studied based on the concept of Lyapunov exponents where the exponents have been estimated using the mathematical model [37]. The estimated Lyapunov exponents will be used as a reference in this work for comparison.

The time series was generated from the mathematical model, of which the simulation program was written using Matlab. The initial conditions were $\theta_0 = \pi/36$ rad, $\dot{\theta}_0 = -0.1$ rad/s. Numerical integration time step-size was $h = 0.0005$ s, the time series included 20,000 data points. The additive Gaussian white noise was then generated and added into the above time series. The noise range was selected from 1 to 5% (40 to 26 dB). The physical parameters and the control gains are listed in Table 1.

Table 1 Physical parameters and control gains of the bipedal robotic system

Body height	$H = 1.78$ m
Body mass	mass $= 80$ kg
Foot-link mass	$m_{\text{f}} = 2 \times 0.0145 \times \text{mass} = 2.32$ kg
Pendulum mass	$m = \text{mass} - m_{\text{f}} = 77.68$ kg
Length of ankle-to-center of mass	$r = 0.575 \times H = 1.02$ m
Foot-link length	$L_{\text{f}} = 0.152 \times H = 0.27$ m
Horizontal ankle-to-heel distance	$a = 0.19 \times L_{\text{f}} = 0.05$ m
Vertical ankle height	$b = 0.039 \times H = 0.07$ m
Horizontal ankle-to-center of foot	$c = 0.5 \times L_{\text{f}} - a = 0.085$ m
Pendulum length	$L = H - b = 1.71$ m
Coefficient of friction	$\mu = 0.5$
Gravity acceleration	$g = 9.80$ m/s^2
Control gain	$K_{\text{p}} = 10000$ Nm
Control gain	$K_{\text{d}} = 2000$ Nms

In estimating Lyapunov exponents based on a time series, some parameters have significant effects on the accuracy of the estimated Lyapunov exponents. Such parameters include the value of the time lag (T_{lag}) which determines the number of the data points to be used in the analysis, as discussed in Sect. 3.1, the evolution time, T_{evol}, and the embedding dimension, d_E. Regarding the time lag (T_{lag}), Taken's results [17] indicate that, in principle, any choice of lags T_{lag} will do. However, if T_{lag} is too small, the coordinates at the successive points in the state space represent almost the same information. On the other hand, if T_{lag} is too large, the successive points represent distinct uncorrelated descriptions of the embedding phase space [25]. Methods have been developed for determining the time lag [27, 39, 40]. In this research, the time lag T_{lag} was determined to be 540 using the first zero crossing of the autocorrelation method [39, 40]. Note that in this work the time lag and evolution time are presented in terms of data points, i.e., the time difference in the number of samples. In terms of time, $T_{\text{lag}} = 540 \times 0.0005 = 0.27$ s.

Another important parameter is the evolution time, T_{evol}. The question of proper selections of the above parameters still remains open. In order to demonstrate that the nonlinear mapping truly improves the accuracy of the estimated Lyapunov exponents and leads to true negative exponents, in this work, the evolution times (T_{evol}) from 100 to 900 were tested, and the best results were found when $T_{\text{evol}} = 600$ (in terms of time, $T_{\text{evol}} = 600 \times 0.0005 = 0.30$ s), of which the results are presented here.

The embedding dimension is another important parameter, especially when estimating Lyapunov exponents using linear mapping. Taken's theorem [17] stated that in order to preserve the dynamical properties of the original attractor, theoretically the embedding dimension should satisfy $d_E \geq 2[d] + 1$, where d is the fractal dimension and $[d]$ is the lowest integer greater than d. In our previous work [14], it has been demonstrated that for the bipedal system investigated here, embedding dimension of 5 has to be used for linear mapping to obtain acceptable negative Lyapunov exponents and dimension of 2 can be used for nonlinear mapping. Note that three spurious Lyapunov exponents will be generated when linear mapping is used. Identifying true exponents is challenging and beyond the scope of this work. Two exponents closest to those from the mathematical model are assumed to be the true ones for comparison. A more detailed discussion on the effects of above important parameters on the accuracy of Lyapunov exponents have been presented in our previous work [14].

3.4.2 Case study 2

In this subsection, we apply our proposed method to the Lorenz system to demonstrate that our method is effective not only for potential stable robotic systems in which all Lyapunov exponents are negative, but also suitable for chaotic systems in which positive, zero, and negative Lyapunov exponents are present.

The Lorenz system:

$$\begin{aligned} \dot{x} &= \sigma(y - x), \\ \dot{y} &= rx - y - xz, \\ \dot{z} &= -bz + xy \end{aligned} \tag{21}$$

was designed to describe convective motion of the Rayleigh–Bénard type, where x is the velocity of the fluid, y is the temperature difference between ascending and descending fluid, and z is the deviation of the temperature profile form linearity [27]. The x component of numerical data for the Lorenz system is created numerically by integrating the Lorenz system with the parameters $\sigma = 16$, $r = 45.92$, and $b = 4.0$ (which have been often used by other researchers [1, 35]) by the fourth-order Runge–Kutta method with a time step $\Delta t = 0.001$. The time series included 20,000 data points. Following the same idea as [35], the additive Gaussian white noise was added into the above time series. Time delay was $T_{\text{lag}} = 4 \times 0.001 = 0.004$ s, $T_{\text{evol}} = 7040 \times 0.001 = 7.04$ s, embedding dimension is selected as 3 used by other researchers [1, 35].

4 Results

We now present our results of Lyapunov exponents estimated from noisy time series for balancing a bipedal robot during standing and the Lorenz system. We compared the effects of four total combinations of two different mappings (linear vs. nonlinear) and two different averaging procedures (Banbrook's [32] and ours as proposed in Sect. 3.3).

4.1 Balancing bipedal robot during standing

Using the parameters listed in Table 1, two Lyapunov exponents were first estimated from the mathematical model with the values of −10.3318 and −18.0704, respectively. Linear mapping was first used for estimating Lyapunov exponents. The averaging method proposed by Banbrook [32], as well as the modified averaging method proposed here, is employed for counteracting the effects of noise. The noise ranges from 1 to 5% (40 to 26 dB). The estimated Lyapunov exponents and their relative errors, with respect to those from the mathematical model, are listed in Table 2 using Banbrook's method [32] and in Table 3 using our proposed averaging method. Tables 2 and 3 show that the relative errors of the exponents determined using both averaging methods are high with the minimum relative error of 53%. This demonstrates that linear mapping is sensitive to the effect of noise, and is not recommended for estimating negative Lyapunov exponents when the time series is contaminated with noise.

The Lyapunov exponents were then estimated using nonlinear mapping with Banbrook's averaging method (Table 4) and the modified averaging method proposed here (Table 5). Table 4 shows that the relative errors between the Lyapunov exponents estimated using nonlinear mapping are below 32% as compared to the minimum relative errors of 53% using linear maps. Table 4 also shows that the minimum relative error for the largest negative exponents is 21.3%, which is significantly higher than the relative errors from the second exponents. Note that the largest Lyapunov exponent is of special interest for stability analysis. The above results demonstrate that nonlinear mapping is less sensitive to the effects of white noise as compared to the linear mapping. However, using the averaging procedure proposed by Banbrook [32], the accuracy of the negative exponents is still dissatisfactory with 25.8 and 12% relative errors for both exponents, even with low level of noise of 1% (signal-to-noise ratio 40 dB).

Table 5 shows the Lyapunov exponents and their relative errors using nonlinear mapping and our proposed modified averaging method. It shows that the relative errors are significantly lower than those using Banbrook's method. To be specific, for the low noise level of 1% (signal-to-noise ratio 40 dB), the relative errors of both exponents are 5.2 and 1.3% as com-

Table 2 Lyapunov exponents and relative errors for the bipedal robotic system with different noise levels using 5D local linear mapping by Banbrook's averaging method ($\lambda_1^* = -10.3318$, $\lambda_2^* = -18.0704$)

Noise%	S/N	λ_4	Error%	λ_5	Error%
5.0	26 dB	−1.7198	83.3543	−5.3881	70.1827
4.0	28 dB	−1.7944	82.6323	−5.3945	70.1473
3.0	30.5 dB	−1.9734	80.8997	−5.4083	70.0709
2.0	34 dB	−2.3555	77.2015	−5.4306	69.9475
1.0	40 dB	−3.1979	69.0480	−5.4802	69.6731

Table 3 Lyapunov exponents and relative errors for the bipedal robotic system with different noise levels using 5D local linear mapping by our averaging method ($\lambda_1^* = -10.3318$, $\lambda_2^* = -18.0704$)

Noise%	S/N	λ_4	Error%	λ_5	Error%
5.0	26 dB	−1.8381	82.2093	−6.2211	65.5730
4.0	28 dB	−1.8566	82.0302	−6.5328	63.8481
3.0	30.5 dB	−1.8756	81.8463	−6.9374	61.6090
2.0	34 dB	−1.9127	81.4873	−7.5007	58.4918
1.0	40 dB	−1.9908	80.7313	−8.4858	53.0403

Table 4 Lyapunov exponents and relative errors for the bipedal robotic system with different noise levels using second-order mapping embedding in 2-dimensional phase space by Banbrook's averaging method ($\lambda_1^* = -10.3318$, $\lambda_2^* = -18.0704$)

Noise%	S/N	λ_1	Error%	λ_2	Error%
5.0	26 dB	−12.5322	21.2974	−13.4367	25.6425
4.0	28 dB	−13.0230	26.0477	−13.8491	23.3603
3.0	30.5 dB	−13.4557	30.2358	−14.5342	19.5690
2.0	34 dB	−13.6091	31.7205	−15.3761	14.9100
1.0	40 dB	−12.9937	25.7641	−15.9049	11.9837

Table 5 Lyapunov exponents and relative errors for the bipedal robotic system with different noise levels using second-order mapping embedding in 2-dimensional phase space by our averaging method ($\lambda_1^* = -10.3318$, $\lambda_2^* = -18.0704$)

Noise%	S/N	λ_1	Error%	λ_2	Error%
5.0	26 dB	−8.5168	17.57	−14.1326	21.79
4.0	28 dB	−8.8449	14.39	−14.7825	18.19
3.0	30.5 dB	−9.2672	10.30	−15.5943	13.70
2.0	34 dB	−9.8426	4.73	−16.6652	7.78
1.0	40 dB	−10.8649	5.16	−18.3048	1.30

Table 6 Lyapunov exponents and relative errors for the Lorenz system with the same noise level using first-order and second-order mapping embedding in 3-dimensional phase space ($\lambda_1^* = 2.16$, $\lambda_2^* = 0.00$, $\lambda_3^* = -32.4$)

		λ_1	Error%	λ_2	Error%	λ_3	Error%
Without noise	1st-order	2.0416	5.48	−0.1728	n/a	−11.8349	63.47
	2nd-order	2.1235	1.69	−0.7566	n/a	−19.0374	41.24
With noise, no average	1st-order	2.0409	5.51	−0.1744	n/a	−11.8342	63.47
	2nd-order	2.1232	1.70	−0.7527	n/a	−19.0747	41.13
With noise, average	1st-order	2.1610	0.046	−0.7275	n/a	−13.4618	58.45
	2nd-order	2.1608	0.037	−0.7747	n/a	−21.1014	34.87

pared to 25.8 and 12% using Banbrook's method. As the noise level increases to 3% (signal-to-noise ratio 30.5 dB), the relative errors of the exponents are still below 15% (10.3 and 13.7%) as compared to 30.2% shown in Table 4. The low relative errors show that the combination of nonlinear mapping and our proposed averaging method for generating the neighbors is effective on counteracting the effects of noise for estimating accurate Lyapunov exponents using noisy time series.

4.2 Lorenz system

With the parameters $\sigma = 16$, $r = 45.92$, and $b = 4.0$ for the Lorenz system shown in (21), three Lyapunov exponents were first estimated from the mathematical model with the values of 2.16, 0.0 and −32.4, respectively, and these values are used as reference in this case study.

The computed Lyapunov exponents' spectrum for the Lorenz system based on time series and their relative errors with respect to those from the mathematical model are listed in Table 6. The first two rows show the estimated Lyapunov exponents and their relative errors for the precision of 10^{-4} of the time series without adding white noise using linear mapping and nonlinear mapping. The following two rows show the results for times series with additive white noise using linear mapping and nonlinear mapping but without applying averaging procedure to compensate for the noise influence. The last two rows show the results for times series with additive white noise using linear mapping and nonlinear mapping, and with averaging procedure to compensate for the noise influence. From Table 6, the first two rows show that nonlinear mapping can achieve a more accurate largest positive exponent (1.69% error versus 5.48%), and a better negative one than linear mapping (41.24 versus 63.47%). When noise was added to the time series without applying the averaging technique, similar observations can be made. Table 6 also shows that when our proposed averaging technique was used, the errors between the exponents from the noisy time series and those from the mathematical model are significantly reduced regardless of the type of mapping. To be specific, when linear mapping is used, the errors for the positive exponents dropped from 5.51 to 0.046%, and for nonlinear mapping, the errors dropped from 1.7 to 0.037%. For negative Lyapunov exponents, the errors dropped from 63.47 to 58.45% using linear mapping, and for nonlinear mapping the errors in negative exponents dropped from 41.13 to 34.87%. It is clear that combining the averaging technique with nonlinear mapping further improves the accuracy of both positive and negative exponents.

5 Discussion

This research is motivated by the fact that existing methods for estimating Lyapunov exponents using a time series are effective for positive exponents, but not reliable for the negative ones. Although for diagnosing chaotic systems positive exponents are of interest, reliable estimation of negative Lyapunov exponents is crucial for the stability analysis when all exponents are negative. Another motivation is that when a time series is collected from experiments, noise measurement is inevitable, especially additive white noise for mechanical systems. Such a noise can have adverse effect on the accuracy of both positive and negative Lyapunov exponents.

We developed a method for estimating Lyapunov exponents using a time series with additive white

noise. The method consists of two key components: (1) nonlinear mapping to determine the neighborhood mapping matrices, and (2) modified averaging procedure based on Banbrook's method [33] to counteract the effect of noise when forming the neighbors. The role of each part, nonlinear mapping versus linear mapping and our proposed modified averaging procedure versus Banbrook's procedure, is systematically examined using two case studies: (a) balancing control of a bipedal robot, and (b) the Lorenz system. The two systems are very different in that for Case I, both Lyapunov exponents are negative and for Case II, all positive, zero and negative exponents are exhibited. It has been found that, as compared with the previous method [33], each individual part of our proposed method improves the accuracy of the Lyapunov exponents. However, it is the combination of both nonlinear mapping and our modified averaging procedure that makes the proposed method robust to the effects of noise.

Another advantage is that by using nonlinear mapping, we can use the reconstructed state space with lower embedding dimensions. In our previous work [14], it has been demonstrated that for the bipedal system investigated here, embedding dimension of 5 has to be used for linear mapping to obtain acceptable Lyapunov exponents and dimension of 2 can be used for nonlinear mapping. This is because, using higher-order mapping, the local neighborhood-to-neighborhood map contains more information of the underlying dynamical system than just using the local linear map, and a more accurate description of the system can be achieved. Thus the embedding dimension of 2 is adequate for estimating Lyapunov exponents using nonlinear mapping. Using lower dimensions of the embedded state space is highly desirable to reduce spurious exponents.

The significance of this work is that, previously, estimating the Lyapunov exponents using a time series has been restricted to chaotic systems, i.e., the largest Lyapunov exponent is positive, which restricts the applications of the concept of Lyapunov exponents to potential stable systems, where the largest Lyapunov exponent is negative. The proposed method, together with our previous work [14], extends the applications of Lyapunov exponents to the analysis of potentially stable systems. Our second case study also shows that our proposed method with nonlinear mapping can also improve the accuracy of positive Lyapunov exponents using noisy time series.

In spite of the promises of the proposed method, there are several limitations. One is that the noise considered in this work is restricted to additive Gaussian white noise. Such a type of noise is for us of interest because it is often encountered in the measurements of mechanical systems and other engineering systems. For other types of noise, such as colored noise, non-uniformly distributed noise and stochastic elements, etc., the applicability of the proposed method has not been explored and remains a future work. In addition, estimation of zero Lyapunov exponents is of great interest for systems with stable limit cycles, which is beyond the scope of this work. Another limitation of the proposed method is the requirement of a large amount of data due to nonlinear mapping. For a short time series, the effectiveness of the proposed method is questionable.

This research is in line with the ongoing research efforts on developing methods for estimating Lyapunov exponents using a time series, of which the quality of the time series might be compromised (noise contamination, length of the time series, etc.). Future work includes the consideration of other types of noise associated with the time series, such as colored noise, non-uniformly distributed noise and stochastic elements, etc. For control systems, controller design has significant effect on the system's qualitative and quantitative performance. Exploring such effects and, in return, the design of stability control based on Lyapunov exponents, is highly desirable to the control community.

Acknowledgements We thank the anonymous reviewers for helpful and insightful remarks. This research is supported by Natural Sciences and Engineering Research Council of Canada (NSERC) and the Mathematics of Information Technology and Complex Systems (MITACS), Canada.

Appendix

When $\alpha, \beta = 1, 2$, (11) can be written as

$$\begin{aligned} Z_1^r(n;T_1) = {} & \partial F_{11} Z_1^r(n;T_0) + \partial F_{12} Z_2^r(n;T_0) \\ & + \frac{1}{2!}\big\{\partial F_{111} Z_1^r(n;T_0) Z_1^r(n;T_0) \\ & + 2\partial F_{112} Z_1^r(n;T_0) Z_2^r(n;T_0) \\ & + \partial F_{122} Z_2^r(n;T_0) Z_2^r(n;T_0)\big\}, \end{aligned} \tag{A1a}$$

$$Z_2^r(n;T_1) = \partial F_{21} Z_1^r(n;T_0) + \partial F_{22} Z_2^r(n;T_0) + \frac{1}{2!}\{\partial F_{211} Z_1^r(n;T_0) Z_1^r(n;T_0) + 2\partial F_{212} Z_1^r(n;T_0) Z_2^r(n;T_0) + \partial F_{222} Z_2^r(n;T_0) Z_2^r(n;T_0)\}. \quad \text{(A1b)}$$

Rewriting (A1) in a matrix form, we have

$$\begin{pmatrix} Z_1^r(n;T_1) \\ Z_2^r(n;T_1) \end{pmatrix} = \begin{bmatrix} J_{11} & J_{12} \\ J_{21} & J_{22} \end{bmatrix} \begin{pmatrix} Z_1^r(n;T_0) \\ Z_2^r(n;T_0) \end{pmatrix}. \quad \text{(A2)}$$

The ten coefficients in (A1) can be determined using the least-squares method, which minimizes the following distance:

$$\Pi = \sum_{i=1}^{N_P} \left\| Z^i(n;T_1) - JZ^i(n;T_0) \right\|^2. \quad \text{(A3)}$$

Since the focus of this work is on the robustness to noise method, the reader is referred to our previous work [14] for detailed description on the procedures of obtaining coefficients a_i, b_i $(i = 1, \ldots, 5)$ (which were derived in detail in Appendix A of [14]), the mapping matrices, and the estimation of the Lyapunov spectra.

References

1. Wolf, A., Swift, J.B., Swinney, H.L., Vastano, J.A.: Determining Lyapunov exponents from a time series. Physics D **16**, 285–317 (1985)
2. Alligood, K.T., Sauer, T.D., Yorke, J.A.: Chaos, an Introduction to Dynamical Systems. Springer, New York (1997)
3. Williams, G.P.: Chaos Theory Tamed. Joseph Henry Press, Washington (1997)
4. Sekhavat, P., Sepehri, N., Wu, Q.: Calculation of Lyapunov exponents using nonstandard finite difference discretization scheme: A case study. J. Differ. Equ. Appl. **10**(4), 369–378 (2004)
5. Müller, P.C.: Calculation of Lyapunov exponents for dynamic systems with discontinuities. Chaos Solitons Fractals **5**, 1671–1681 (1995)
6. Oseledec, V.I.: A multiplicative ergodic theorem: Lyapunov characteristic numbers for dynamical systems. Trans. Mosc. Math. Soc. **19**, 197 (1968)
7. Asokanthan, S.F., Wang, X.H.: Characterization of torsional instability in a Hooke's joint driven system via maximal Lyapunov exponents. J. Sound Vib. **194**(1), 83–91 (1996)
8. Gilat, R., Aboudi, J.: Parametric stability of non-linearly elastic composite plates by Lyapunov exponents. J. Sound Vib. **235**(4), 627–637 (2000)
9. Zevin, A.A., Pinsky, M.A.: Absolute stability criteria for a generalized Lur'e problem with delay in the feedback. SIAM J. Control Optim. **43**(6), 2000–2008 (2005)
10. Awrejcewicz, J., Kudra, G.: Stability analysis and Lyapunov exponents of a multi-body mechanical system with rigid unilateral constraints. Nonlinear Anal. Theory Methods Appl. **63**, 909–918 (2005)
11. Rogelio, C., Gustavo, A., Javier, C.P.: Determination of limit cycles using both the slope of correlation integral and dominant Lyapunov methods. Nuclear Technol. **145**(2), 139–149 (2004)
12. Wu, Q., Sekhavat, P., Sepehri, N., Peles, S.: On design of continuous Lyapunov's feedback control. J. Franklin Inst. Eng. Appl. Math. **342**(6), 702–723 (2005)
13. Sekhavat, P., Sepehri, N., Wu, Q.: Impact control in hydraulic actuators with friction: Theory and experiments. IFAC J. Control Eng. Pract. **14**(12), 1423–1433 (2006)
14. Yang, C., Wu, Q.: On Stability analysis via Lyapunov exponents calculated from a time series using nonlinear mapping—a case study. Nonlinear Dyn. **59**(1), 239–257 (2009)
15. Ghorbani, R., Wu, Q.: Optimal neural network stabilization of bipedal robots using genetic algorithm. Eng. Appl. Artif. Intell. **20**, 473–480 (2007)
16. Yang, C., Wu, Q.: On stabilization of bipedal robots during disturbed standing using the concept of Lyapunov exponents. Robotica **24**, 621–624 (2006)
17. Takens, F.: In: Rand, D.A., Young, L.-S. (eds.) Dynamical Systems and Turbulence. Lecture Notes in Mathematics, vol. 898. Springer, Berlin (1981)
18. Yasuaki, O., Muhammad, A., Akihiro, S., Kazuki, F., Hikaru, I., Ryoichi, N., Ichiro, T.: Assessment of walking stability of elderly by means of nonlinear time-series analysis and simple accelerometry. JSME Int. J., Ser. C: Mech. Syst. Mach. Elements Manuf. **48**(4), 607–612 (2006)
19. Burdet, E., Tee, K.P., Mareels, I., Milner, T.E., Chew, C.M., Franklin, D.W., Osu, R., Kawato, M.: Stability and motor adaptation in human arm movements. Biol. Cybern. **94**(1), 20–32 (2006)
20. Dingwell, B.J., Cusumano, J.P.: Nonlinear time series analysis of normal and pathological human walking. Chaos **10**(4), 848–863 (2000)
21. Dingwell, J.B., Cusumano, J.P., Sternad, D., Cavanagh, P.R.: Slower speeds in patients with diabetic neuropathy lead to improved local dynamic stability of continuous overground walking. J. Biomech. **33**, 1269–1277 (2000)
22. Dingwell, J.B., Cusumano, J.P., Cavanagh, P.R., Sternad, D.: Local dynamic stability versus kinematic variability of continuous overground and treadmill walking. ASME J. Biomech. Eng. **123**, 27–32 (2001)
23. Dingwell, J.B., Marin, L.C.: Kinematic variability and local dynamic stability of upper body motions when walking at different speeds. J. Biomech. **39**, 444–452 (2006)
24. Dingwell, B.J.: Lyapunov Exponents. Wiley Encyclopedia of Biomedical Engineering. Wiley, New York (2006)
25. Sano, M., Sawada, Y.: Measurement of the Lyapunov spectrum from chaotic time series. Phys. Rev. Lett. **55**, 1082 (1985)
26. Kunze, M.: Non-Smooth Dynamical Systems. Springer, Berlin (2000)
27. Kantz, H., Schreiber, T.: Nonlinear Time Series Analysis, 2nd edn. Cambridge University Press, Cambridge (2004)

28. Zeng, X., Eykholt, R., Pielke, R.A.: Estimating the Lyapunov-exponent spectrum from short time series of low precision. Phys. Rev. Lett. **66**(25), 3229–3232 (1991)
29. Zeng, X., Pielke, R.A., Eykholt, R.: Extracting Lyapunov exponents from short time series of low precision. Mod. Phys. Lett. B **6**(2), 55–75 (1992)
30. Rosenstein, M.T., Collins, J.J., DeLuca, C.J.: A practical method for calculating largest Lyapunov exponents from small data sets. Phys. D: Nonlinear Phenom. **65**, 117–134 (1993)
31. Hegger, R., Kantz, H., Schreiber, T.: Practical implementation of nonlinear time series analysis: The TISEAN package. Chaos Interdiscip. J. Nonlinear Sci. **9**(2), 413–435 (1999)
32. Kantz, H.: A robust method to estimate the maximal Lyapunov exponent of a time series. Phys. Lett. A **185**(1), 77–87 (1994)
33. Banbrook, M., Ushaw, G., McLaughlin, S.: How to extract Lyapunov exponents from short and noisy time series. IEEE Trans. Signal Process. **45**(5), 1378–1382 (1997)
34. Darbyshire, A.G., Broomhead, D.S.: Robust estimation of tangent maps and Lyapunov spectra. Physica D **89**, 287–305 (1996)
35. Brown, R., Bryant, P., Abarbanel, H.D.: Computing the Lyapunov spectrum of a dynamical system from an observed time series. Phys. Rev. A **43**, 2787–2806 (1991)
36. Holzfuss, J., Lauterborn, W.: Lyapunov exponents from a time series of acoustic chaos. Phys. Rev. A **39**, 2146–2152 (1989)
37. Yang, C., Wu, Q.: Effects of constraints on bipedal balance control. In: Proceedings of the 2006 American Control Conference, Minneapolis, MN, June 14–16, pp. 2510–2515 (2006)
38. Vukobratović, M., Borovać, B.: Zero-moment point—thirty years of its life. Int. J. Humanoid Robot. **1**(1), 157–173 (2004)
39. Abarbanel, H.D.I., Brown, R., Kennel, M.B.: Local Lyapunov exponents computed from observed data. J. Nonlinear Sci. **2**, 343–365 (1992)
40. Abarbanel, H.D.I., Brown, R., Kennel, M.B.: Prediction in chaotic nonlinear systems: Methods for time series with broadband Fourier spectra. J. Nonlinear Sci. Phys. Rev. A **41**(4), 1782–1807 (1990)